

Supplementary Information for “Black hole information turbulence and the Hubble tension”

Juan Luis Cabrera Fernández^{1,2,*}

¹Departamento de Física Aplicada, ETSI Aeronáutica y del Espacio, Universidad Politécnica de Madrid, Pza. Cardenal Cisneros 3, 28040, Madrid, Spain.

²Laboratorio de Dinámica Estocástica, Centro de Física, Instituto Venezolano de Investigaciones Científicas, Caracas 1020-A, Venezuela.

*juanluis.cabrera[at]upm.es

ABSTRACT

This is the Supplementary Information file for the article “Black hole information turbulence and the Hubble tension”.

An illustrative example of the leading term at generation $\tau = 3$ of the eigenvalues governing the dynamics of the population of qubits

The leading term at generation $\tau = 3$ is called here Λ_3 . We can grasp how the eigenvalues behave by observing the way the term Λ_3 is assembled (see¹ for the meaning of α and β),

$$\Lambda_3 \equiv \left\{ \begin{array}{l} \left[\begin{array}{l} (1 + \beta^2 \alpha^2) r_1^2 \\ + (\beta^2 + \beta^4 \alpha^2) \end{array} \right] r_2^2 \\ + \left[\begin{array}{l} (-2\alpha\beta^2 - 2\beta^4\alpha^3) r_1^2 \\ + (\beta^4\alpha^2 + \beta^6\alpha^4) r_1^2 \end{array} \right] r_2 \end{array} \right\} r_3^2 \quad (1)$$

$$+ \left\{ \begin{array}{l} \left[\begin{array}{l} (-2\alpha\beta^2) r_1^2 \\ + (-2\alpha\beta^4) \end{array} \right] r_2^2 \\ + \left[\begin{array}{l} (2\alpha^2\beta^4) r_1^2 \end{array} \right] r_2 \end{array} \right\} r_3$$

$$+ \left\{ \begin{array}{l} \left[\begin{array}{l} (\beta^4\alpha^2) r_1^2 \\ + (\alpha^2\beta^6) \end{array} \right] r_2^2 \end{array} \right\}$$

The nested coefficients structures a cascade as illustrated in the main text Fig. 1. Given the initial coefficient values for the second order term: $C_2 = 1 + \beta^2 \alpha^2$, the linear term: $C_1 = 0$, and the independent term: $C_0 = \beta^2$; the generation rule allow us to calculate the coefficients that will form the leading term of the eigenvalues at the next iteration $\tau = 2$, shown in the second row of the main text Fig. 1. Now, this new set of coefficients allows for the calculation of the nested coefficients of the leading term of the eigenvalues at the iteration $\tau = 3$ (third row at the same figure); a full cascade is generated by iteratively applying the generation rule. On each iteration τ , 3^τ new terms are generated.

The generation rule

The coefficients of higher order values of the leading term can be precisely obtained from the preceding terms by the following generation rule. In general, if we know Λ_1 and Λ_2 , we can obtain Λ_τ given that, in the generation $\tau - 1$, the term $\{C_2 r_i^2 + C_1 r_i + C_0\} r_{i+1}^k$, with $k = 0, 1, 2$; generates the polynomial

$$\left\{ \begin{array}{l} [C_2 r_i^2 + C_1 \chi_1 r_i + \beta^2 C_2] r_{i+1}^2 \\ + [-k\alpha\beta^2 C_2 r_i^2 + C_1 \chi_2 r_i + C_1 \chi_3] r_{i+1} \\ + [\beta^2 \alpha^2 C_0 r_i^2 + C_1 \chi_4 r_i + C_1 \chi_5] \end{array} \right\} r_{i+2}^k, \quad (2)$$

in the next generation τ . There is no need to determine the unknowns, $\chi_1, \chi_2, \dots, \chi_5$, because in the current situation $C_1 = 0$ (see details in¹).

28 Fractal construction

29 The structure of the Λ_τ 's is better represented by the induced fractal it generates: to the initial coefficient values C_2 ,
 30 C_1 and C_0 , same size segments on the unit interval are assigned. After repeated iterations each subset is divided
 31 by a factor of 3, and the newly generated coefficients obtained with the generation rule updates the new $N_\tau = 3^\tau$
 32 subintervals. A detailed account of the process is available at¹.

33 Fitting the cascade's components

Figure 3 shows the number of coloured n_C and lacunar n_L components in the inverted cascade. Both quantities grow exponentially following fits:

$$n_C(\tau) \sim 0.812 e^{0.807 \tau} \quad (3)$$

$$n_L(\tau) \sim 0.561 e^{1.142 \tau} \quad (4)$$

34 One may try to fit the fraction of the cascade coloured, N_C , and lacunar, N_L , components with the equations describing
 35 the fractional energy density of nonrelativistic matter and dark energy. Such a fitting is exemplified by the arbitrary
 36 selection of the following models:

- The consensus cold dark matter model (Λ CDM) :

$$N_L(\tau) = \frac{p_m(1+C_z\tau)^3}{p_r(1+C_z\tau)^4 + p_m(1+C_z\tau)^3 + p_k(1+C_z\tau)^2 + (1-p_k-p_m-p_r)} \quad (5)$$

- The constant w model (w CDM) :

$$N_L(\tau) = \frac{p_m(1+C_z\tau)^3}{p_r(1+C_z\tau)^4 + p_m(1+C_z\tau)^3 + p_k(1+C_z\tau)^2 + (1-p_k-p_m-p_r)(1+C_z\tau)^\omega} \quad (6)$$

- The Chevallier–Polarski–Linder model (CPL):

$$N_L(\tau) = \frac{p_m(1+C_z\tau)^3}{p_r(1+C_z\tau)^4 + p_m(1+C_z\tau)^3 + p_k(1+C_z\tau)^2 + (1-p_k-p_m-p_r)(1+C_z\tau)^{3(1+\omega_0+\omega_a)} e^{\frac{-3\omega_a C_z \tau}{1+C_z \tau}}} \quad (7)$$

- The generalised Chaplygin gas model (GCG):

$$N_L(\tau) = \frac{p_m(1+C_z\tau)^3}{p_r(1+C_z\tau)^4 + p_b(1+C_z\tau)^3 + p_k(1+C_z\tau)^2 + (1-p_k-p_b-p_r)[(A_s + (1-A_s)(1+C_z\tau)^{3(1+\alpha)})^{\frac{1}{1+\alpha}}]} \quad (8)$$

- The interacting dark energy model (IDE):

$$N_L(\tau) = \frac{p_m(1+C_z\tau)^3}{p_r(1+C_z\tau)^4 + p_k(1+C_z\tau)^2 + (1-p_k-p_m-p_r)(1+C_z\tau)^{3(1+\omega_x)} + \frac{b_m}{\delta+3\omega_x}[\delta(1+C_\tau)^{3(1+\omega_x)} + 3\omega_x(1+C_z\tau)^{3-\delta}]} \quad (9)$$

- Early dark energy model (EDE)

$$N_L(\tau) = \frac{p_m(1+C_z\tau)^3(1-\Omega_{DE}(z))}{p_r(1+C_z\tau)^4 + p_m(1+C_z\tau)^3 + p_k(1+C_z\tau)^2} \quad (10)$$

$$\begin{aligned} \Omega_{DE}(z) \equiv & ((1.0 - p_k - p_m - p_r) - w_e(1 - (1 + C_z\tau)^{3w_0})) \\ & \times [(1.0 - p_k - p_m - p_r) + p_k(1 + C_z\tau)^{-3w_0-1} \\ & + p_m(1 + C_z\tau)^{-3w_0} + p_r(1 + C_z\tau)^{-3w_0+1}]^{-1} \\ & + w_e(1 - (1 + C_z\tau)^{3w_0}). \end{aligned} \quad (11)$$

- Poulin *et al.* Early Dark Model (EDEP)

$$N_L(\tau) = \frac{p_m(1 + C_z\tau)^3}{p_r(1 + C_z\tau)^4 + p_m(1 + C_z\tau)^3 + p_k(1 + C_z\tau)^2 + (1.0 - p_k - p_m - p_r) + \frac{2p_a}{\left(\frac{1 + Z^c}{1 + C_z\tau}\right)^{3(w_n+1)} + 1}} \quad (12)$$

and $N_C(\tau) = 1 - N_L(\tau)$ for all the cases.

With the exception of $\Omega_{DE}(\tau)$ - being a function - we avoided the conventional use of the sign for the energy densities (Ω_x) as - at this point in our discourse -, the fitting parameters have no physical meaning. Even so, we have kept the same subscripts to maintain a certain parallelism with the original meaning, i.e., we deal with parameters p_k, p_m, p_r in the Λ CDM model. The w CDM adds the parameter w , the CPL, GCG, IDE and EDE models include the additional parameter sets (ω_0, ω_a) , (A_s, α) , (ω_x, δ) and (ω_0, Ω_e) , respectively, while the EDEP includes the parameters (p_a, w_n, Z^c) . Used models where inspired by³ where all of them included a contribution from curvature. In particular, the EDE model is based on^{4,5}. However the EDEP model was assembled using equations (5) and (15) in⁶ and, for fitting purposes, we decided to took the previous triple as parameters. We incorporated the additional parameter C_z which intents to fit the relationship between the iteration step τ and the cosmological redshift z . Best fit parameters using the Turing.jl package for Bayesian inference with the No-U-Turn sampler⁷ are summarised in Table 1 and the corner plots for the parameters and their covariance are shown in Figs. 3-8. No corner plot for the GCG model are included as our fitting results were quite unsatisfactory. With the exception of GCG all the models yielded a σ^2 measure of the order of $\sim 10^{-4}$ with w CDM reaching a best value of $\sim 10^{-5}$. For all the models $p_\Lambda \sim 0.8$ and p_m is in the range $\sim 0.14 - 0.18$. While GCG differs substantially, most models produced $p_k \sim 0.00027$, excepting EDE with $p_k \sim 0.005726$ and EDEP with the only slightly negative value $p_k \sim -0.001418$ (positive in the error margin, reported in the Fig. 8.). Meanwhile, w CDM, CPL, GCG and IDE reported p_r negative values in the range $\sim [-5.8, -0.2] \times 10^{-3}$, while Λ CDM, EDE and EDEP models have positive $p_r \sim 0.000137, 0.000209$ and 0.000148 (whose σ^2 were $0.000228, 0.000181$ and 0.000226 , respectively). The obtained values for the parameter pairs (ω_0, ω_a) , (A_s, α) and (ω_x, δ) in the CPL, GCG and IDE models are very close to those obtained in³ - i.e., $(-0.966, 0.202)$, $(0.733, -0.011)$ and $(-1.001, -0.0043)$, respectively -¹. Given that the only models yielding positive values for p_r are the Λ CDM, EDE and EDEP models we conclude these are the ones best fitting the N_L data. Remarkably, the best values obtained for the parameter C_z for these models are quite close to each other: $0.365496, 0.389605$ and 0.361704 . Thus, the relationship between iteration steps and the redshift may be written as $z \sim C_z\tau$. Plots with the fitting results for the Λ CDM, w CDM, CPL, IDE, EDE and EDEP models are shown in the Fig. 13.

$E(z)$ used in the calculations of the Hubble constant

The analysis was restricted to the best behavior models from the above section, i.e., $E(\tau)$,

- for the Λ CDM model is given by,

$$E(\tau) = p_r(1 + C_z\tau)^4 + p_m(1 + C_z\tau)^3 + p_k(1 + C_z\tau)^2 + (1 - p_k - p_m - p_r), \quad (13)$$

- for the EDE model is given by,

$$E(\tau) = \frac{p_r(1 + C_z\tau)^4 + p_m(1 + C_z\tau)^3 + p_k(1 + C_z\tau)^2}{1 - \Omega_{DE}(\tau)}, \quad (14)$$

with $\Omega_{DE}(\tau)$ expressed by eq. (11), and

¹³ makes use of data from the Union2.1 SNe compilation and the WiggleZ BAO measurements, together with the WMAP 7-yr distance priors and the observational Hubble data.

- for the EDEP model is given by,

$$E(\tau) = p_r(1 + C_z\tau)^4 + p_m(1 + C_z\tau)^3 + p_k(1 + \tau)^2 + (1.0 - p_k - p_m - p_r) + \frac{2p_a}{\left(\frac{1 + Z^c}{1 + C_z\tau}\right)^{3(w_n+1)} + 1}. \quad (15)$$

The parameter values in these models are those given in Table 1.

H_0 error determination

Native Interpolations.jl doesn't provide built-in confidence intervals. To calculate an error estimation for H_0 we took the mean value of the propagated error of the equation (28) in the main text, i.e.,

$$\varepsilon(H_0) \sim \langle \varepsilon(\Upsilon_x) \rangle = \frac{1}{2} \frac{\varepsilon(p_h)}{p_h} + \frac{1}{2} \left\langle \frac{\varepsilon(\mathcal{M}_x)}{\mathcal{M}_x} \right\rangle. \quad (16)$$

In this expression $\varepsilon(\mathcal{M}_x)$ is the root mean square deviation, i.e. $\varepsilon(\mathcal{M}_x) \equiv \sqrt{\left\langle \left(\frac{\Delta D_x}{D_x} - \mathcal{M}_x^{1/2} \right)^2 \right\rangle}$. Note that

$\varepsilon\left(\frac{\Delta D_x}{D_x}\right) = 0$, as the involved quantities were measured directly on the fractal.

Parameter	ΛCDM	wCDM	CPL	GCG	IDE	EDE	EDEP
C_z	0.366038	0.728667	0.423091	0.917701	0.528297	0.389605	0.361704
p_k	0.000268	0.00027	0.00027	0.334792	0.00027	0.005726	-0.001418
p_m	0.177603	0.141675	0.164878	$p_b \equiv 0.0451$	0.163759	0.179941	0.180455
p_r	0.000137	-0.000225	-0.00035	-0.005757	-0.000459	0.000209	0.000148
p_Λ	0.821993	0.85828	0.835201	0.77703	0.821993	0.814124	0.820815
p_5	—	0.821767	-1.006021	0.747408	-0.822978	-0.953692	0.219839
p_6	—	—	0.205858	-0.011034	-0.00453	0.814125	0.565335
p_7	—	—	—	—	—	—	10^6
σ^2	0.000228	0.000097	0.000126	0.432337	0.000134	0.000181	0.000226

Table 1. Best fit parameters obtained using Julia's Turing.jl Bayesian inference. Here $p_\Lambda \equiv 1 - p_k - p_m - p_r$; $p_5 = w$ in the wCDM, (p_5, p_6) are (ω_0, ω_a) , (A_s, α) , (ω_x, δ) and (ω_0, Ω_e) in the CPL, GCG, IDE and EDE models, respectively; the EDEP model extra parameters are $(p_5, p_6, p_7) = (p_a, w_n, Z^c)$; σ^2 means residuals. In the GCG model p_m was substituted by the present density parameter of baryonic matter $p_b = \Omega_b = 0.0451$, according to the WMAP 7yr results⁹ following the example in³.

Model	D_x	p_h	p_e	H_0
Λ CDM	D_{cg}	116.11 ± 20.21	1.54 ± 0.03	62.79 ± 5.48
Λ CDM	D_m	74.00 ± 0.00	1.41 ± 0.00	70.07 ± 0.09
EDE	D_{cg}	127.87 ± 2.87	1.50 ± 0.04	78.91 ± 0.91
EDE	D_m	35.69 ± 1.23	1.50 ± 0.01	37.57 ± 0.69
EDEP	D_{cg}	134.60 ± 9.99	1.52 ± 0.01	73.55 ± 2.75
EDEP	D_m	39.81 ± 1.08	1.51 ± 0.00	36.91 ± 0.53

Table 2. Best fitted parameters for models given by the equation (21). Bayesian inference with a Markov Chain Monte Carlo and 300000 priors. H_0 was obtained from the estimate posterior distributions according to equations (28) and (29). Zero errors means they are smaller than 10^{-2} . Results for H_0 are in units of $H(\tau)$, i.e. in Km/s/Mpc, as expected.

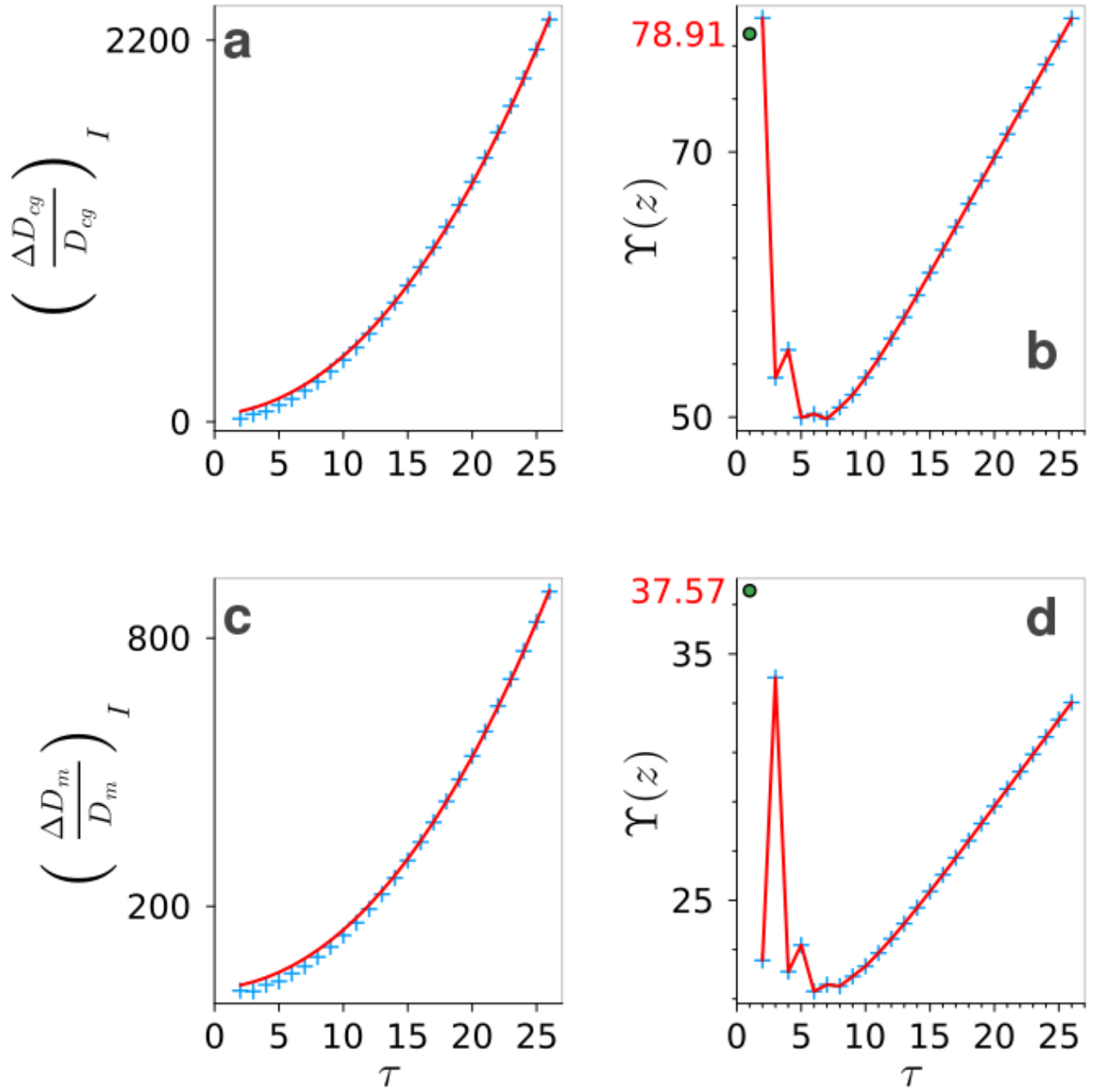


Figure 1. Determination of the Hubble constant from the relative growth of the fractal space. Same as in the main text Fig. 7, but using EDE $E(t)$, i.e., given by the SI equation 14. In this case **b** $H_0 = \Upsilon(1) \sim (78.91 \pm 0.91)$ Km/s/Mpc and **d** $H_0 = \Upsilon(1) \sim (37.57 \pm 0.69)$ Km/s/Mpc.

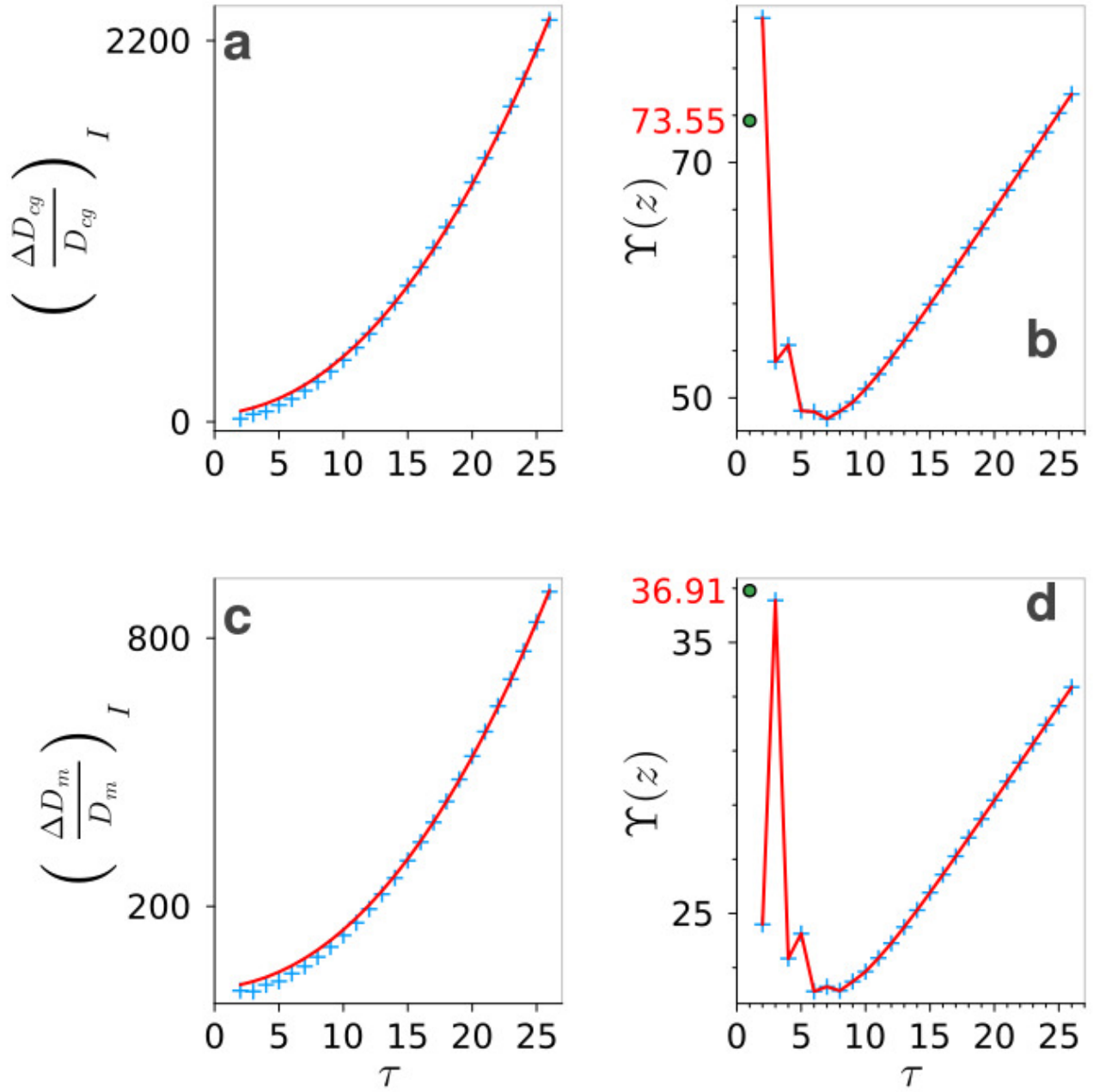


Figure 2. Determination of the Hubble constant from the relative growth of the fractal space. Same as in the main text Fig. 7, but using EDEP $E(t)$, i.e., given by the SI equation 15. In this case **b** $H_0 = \Upsilon(1) \sim (73.55 \pm 2.75)$ Km/s/Mpc and **d** $H_0 = \Upsilon(1) \sim (36.91 \pm 0.53)$ Km/s/Mpc.

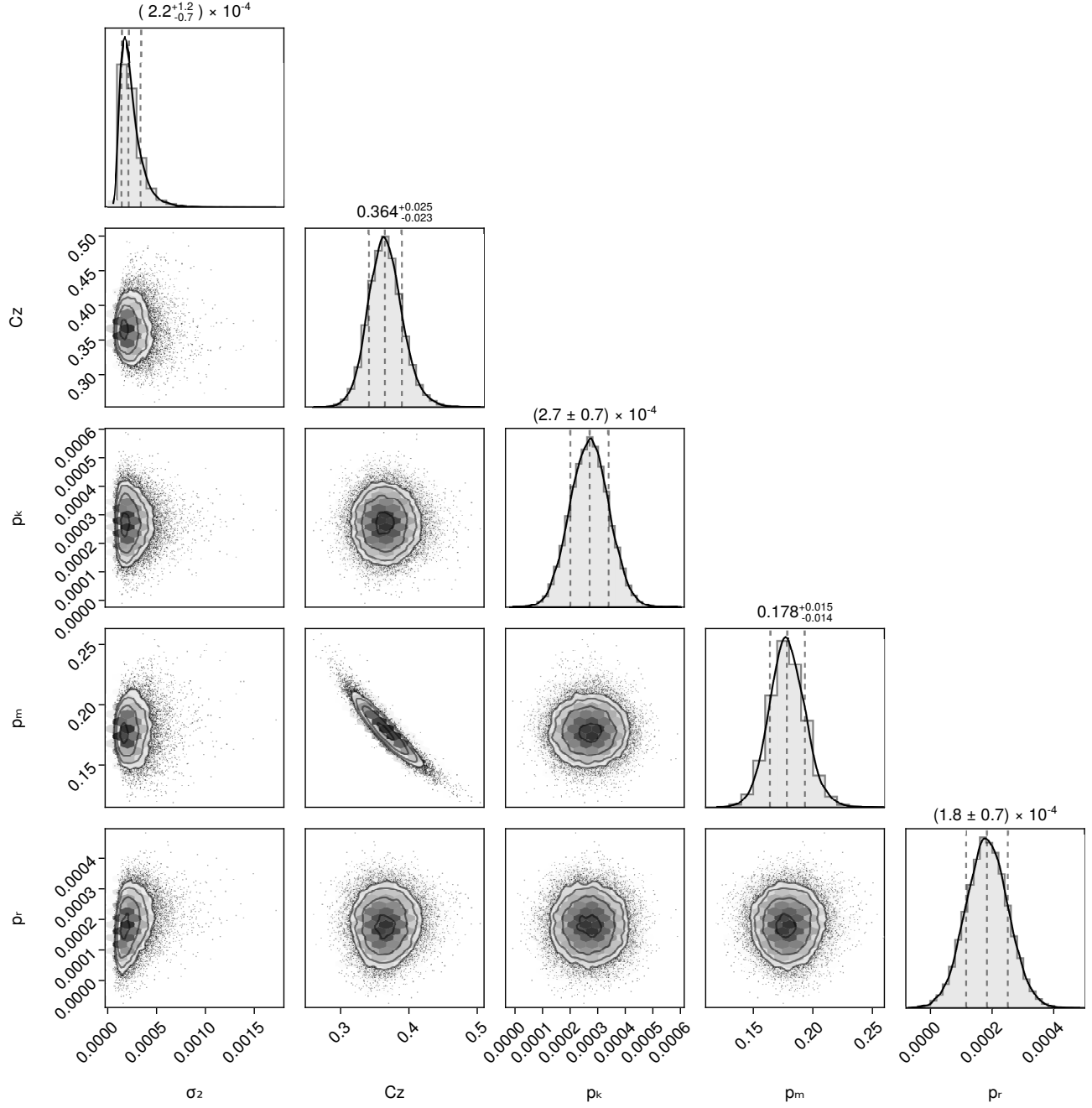


Figure 3. Parameters distribution and their covariance for the Λ CDM model.

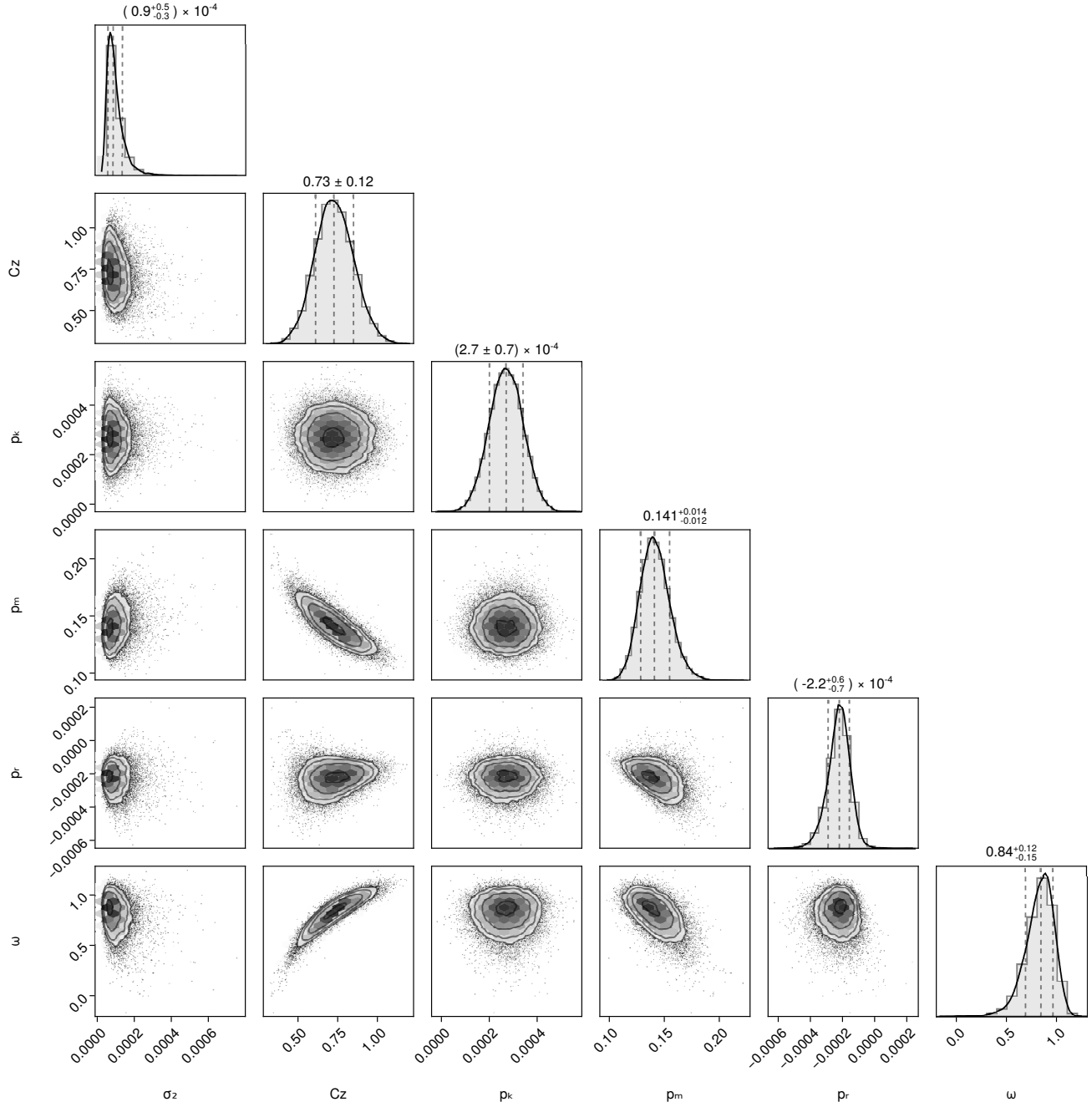


Figure 4. Parameters distribution and their covariance for the w CDM model.

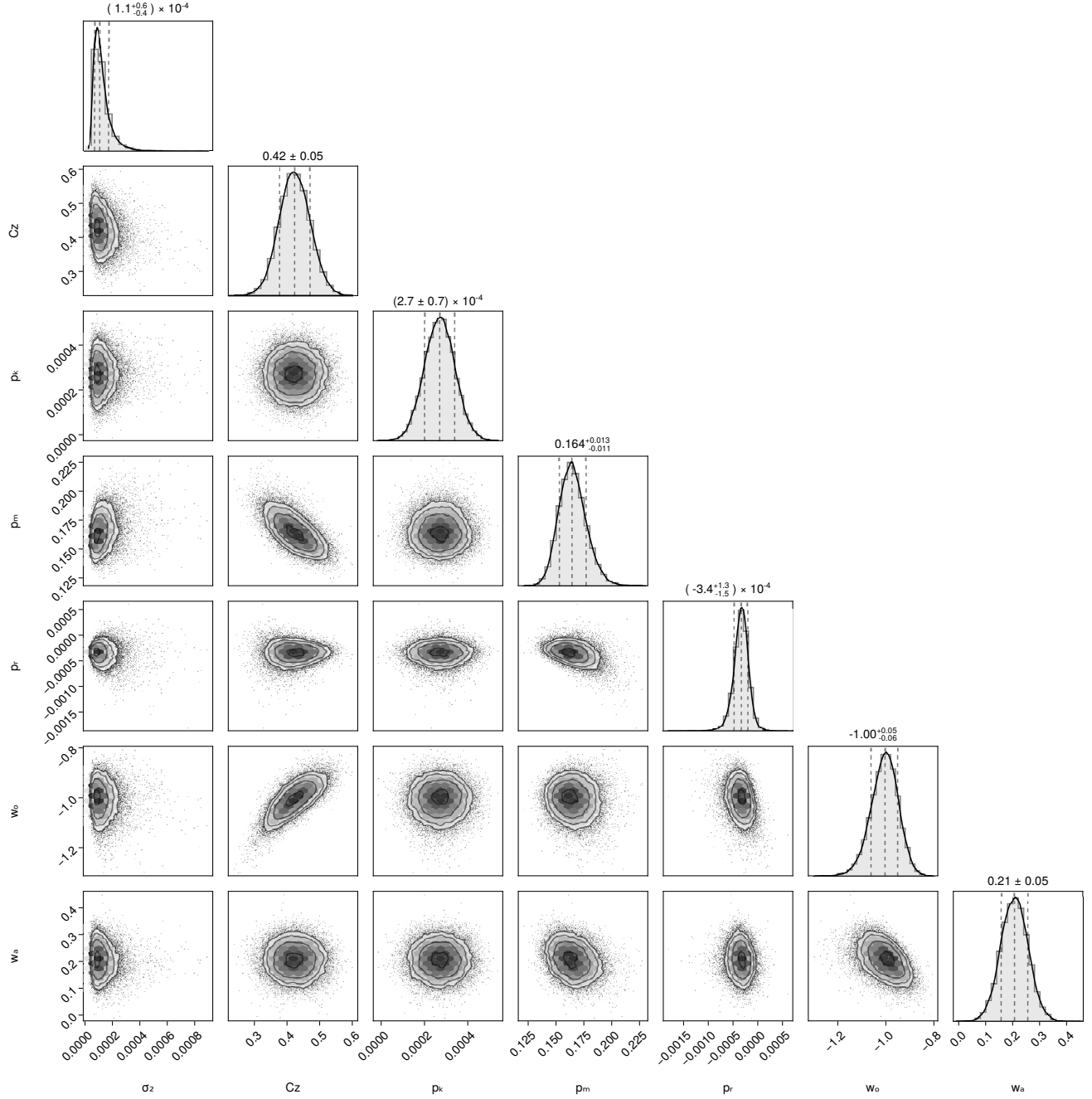


Figure 5. Parameters distribution and their covariance for the CPL model.

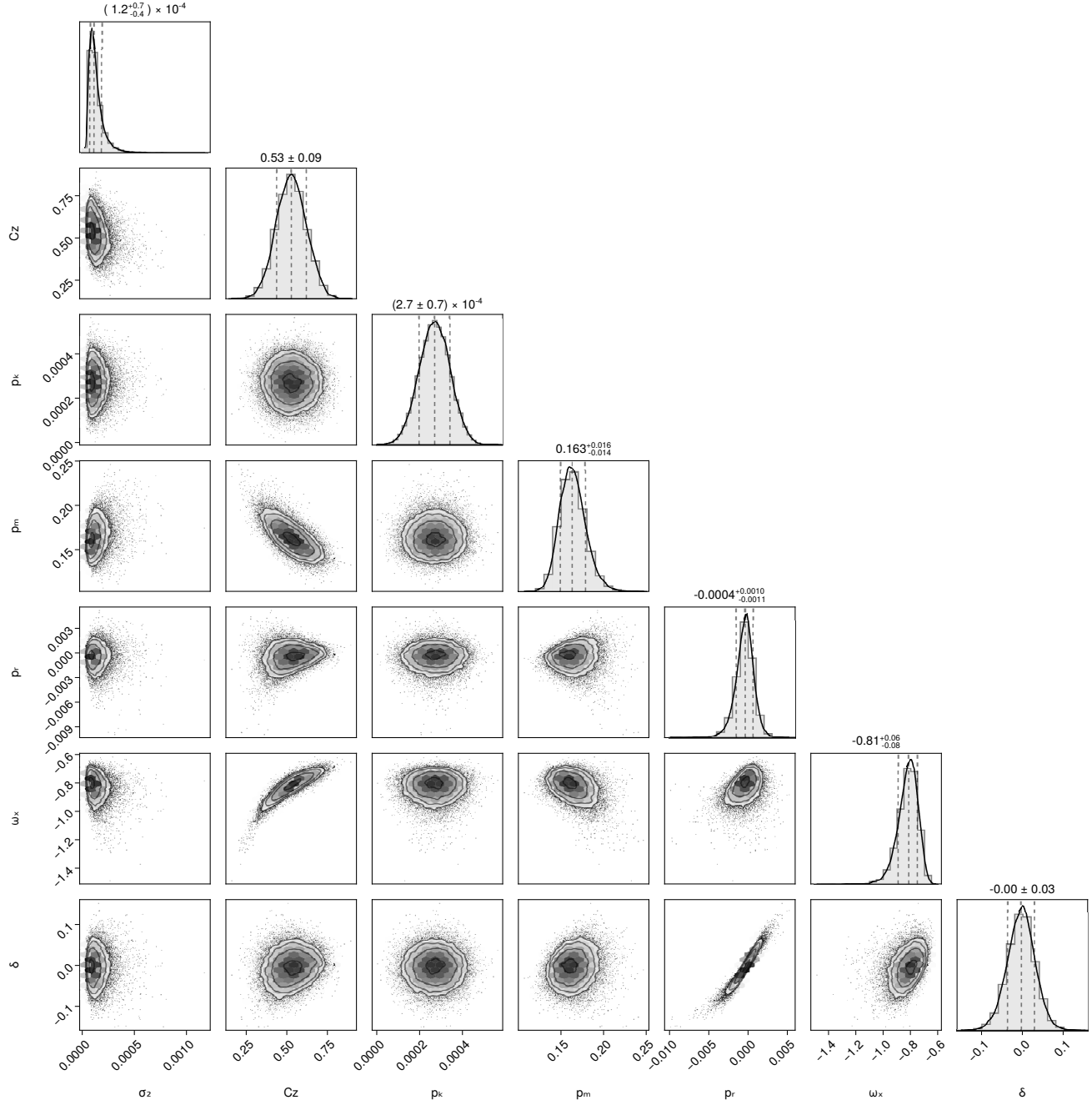


Figure 6. Parameters distribution and their covariance for the IDE model.

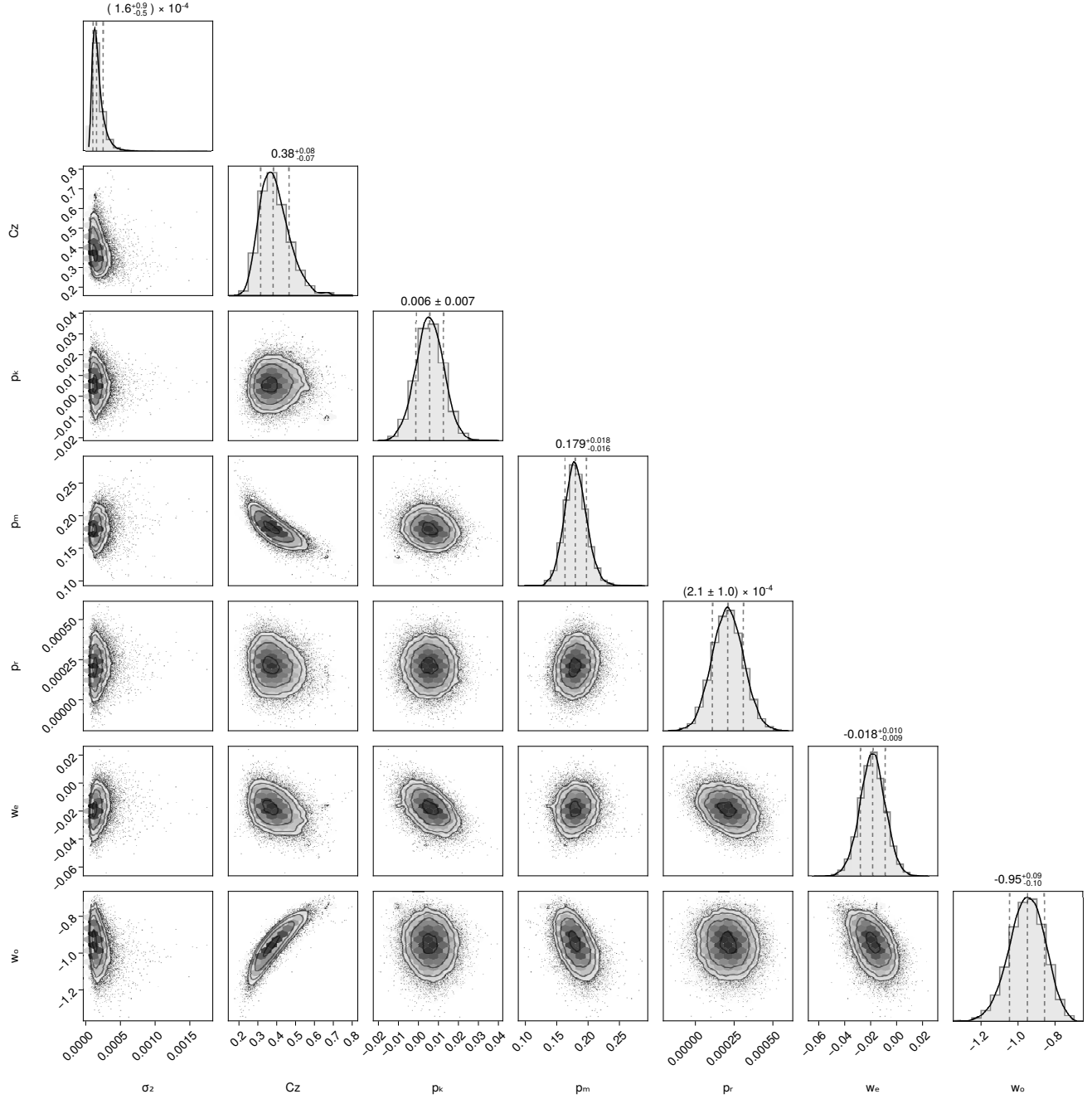


Figure 7. Parameters distribution and their covariance for the EDE model.

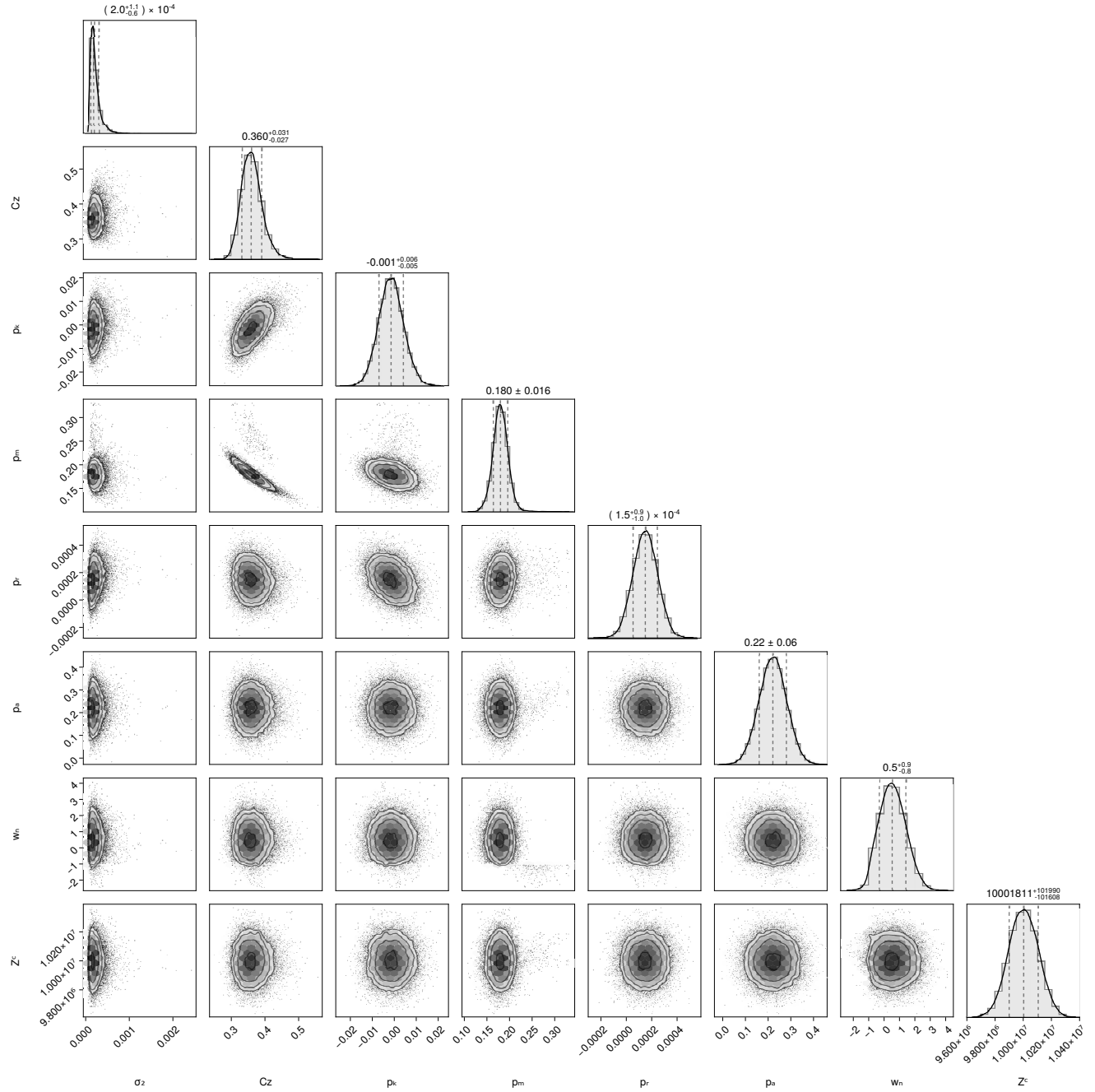


Figure 8. Parameters distribution and their covariance for the EDEP model.

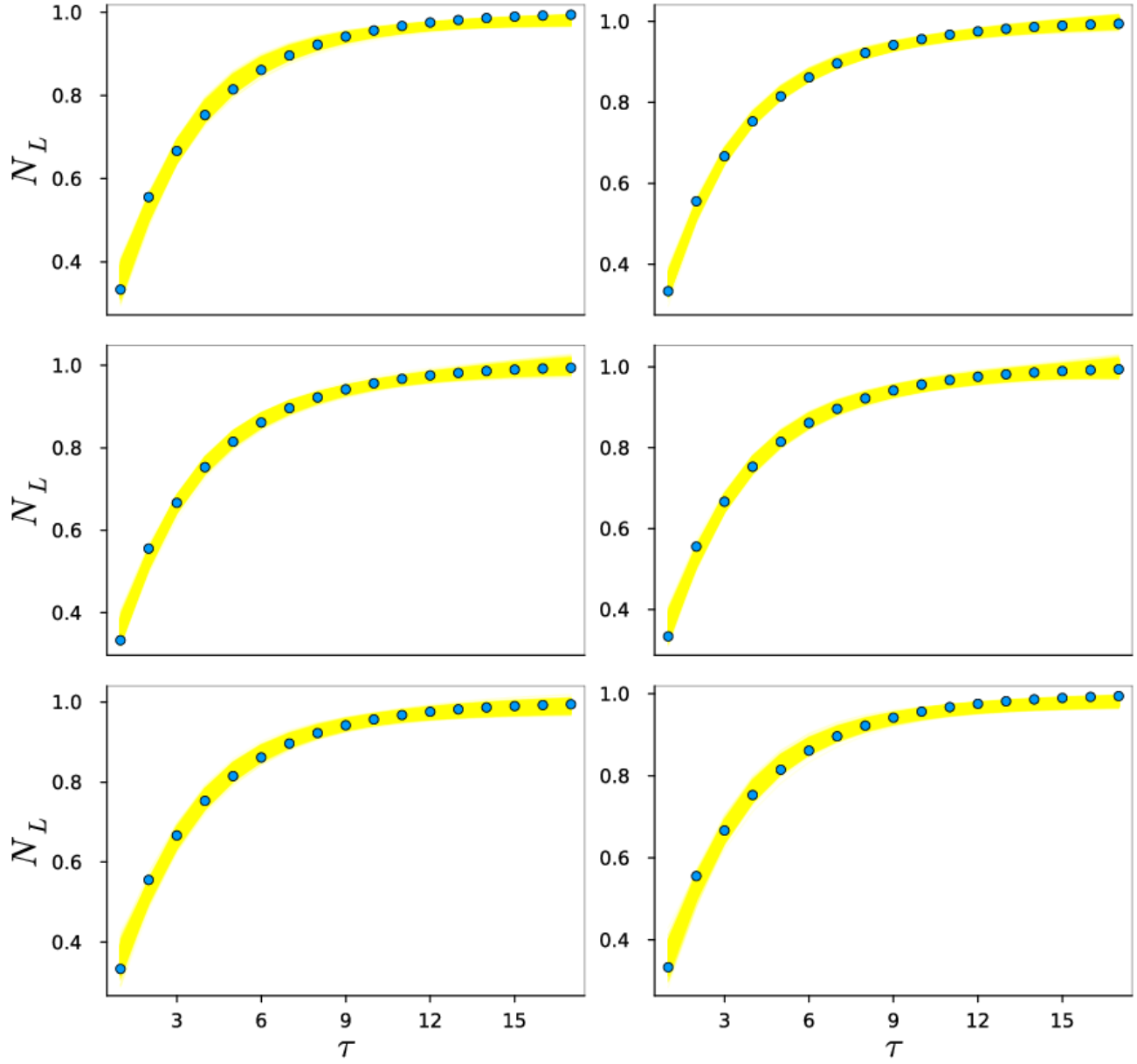


Figure 9. All cosmological models fitting. From left to right and from top to bottom Λ CDM, w CDM, CPL, IDE, EDE and EDEP models fitted using Julia's Turing.jl Bayesian inference.

70 References

- 71 **1.** Cabrera J. L., Gutiérrez D. E. & Rodríguez M., Criticality and the fractal structure of $-5/3$ turbulent cascades.
72 Chaos, Solitons and Fractals **146** 110876 (2021).
- 73 **2.** Komatsu, E. et al., Seven-Year Wilkinson Microwave Anisotropy Probe (WMAP*) Observations: Cosmological
74 Interpretation. The Astrophysical Journal Supplement Series **192**, 18 (2011)
- 75 **3.** Shi, K., Huang, Y. F. & Lu, T., A comprehensive comparison of cosmological models from the latest observational
76 data. Monthly Notices of the Royal Astronomical Society **426**, 2452-2462 (2012).
- 77 **4.** Doran, M., Schwindt, J-M., & Wetterich, C., Structure formation and the time dependence of quintessence. Phys.
78 Rev. D **64** 123520 (2001).
- 79 **5.** Doran, M. & Robbers, G., Early dark energy cosmologies. Journal of Cosmology and Astroparticle Physics **6**
80 026 (2006).
- 81 **6.** Poulin, V., Smith T. L., Grin D., Karwal T. & Kamionkowski, M., Cosmological implications of ultralight
82 axionlike fields. Phys. Rev. D **98** 083525 (2018).
- 83 **7.** Hoffman, M. D. & Gelman, A., vJournal of Machine Learning Research **15**, 1593-1623 (2014).
- 84 **8.** Salahedin, F., Pazhouhesh, R., Malekjani, M.. Cosmological constraints on new generalized Chaplygin gas model.
85 Eur. Phys. J. Plus **135**, 429 (2020).
- 86 **9.** Komatsu, E. et al., Seven-Year Wilkinson Microwave Anisotropy Probe (WMAP*) Observations: Cosmological
87 Interpretation. The Astrophysical Journal Supplement Series **192**, 18 (2011)